Tutor/s

Dr. José Fermín López Sánchez
Departament d'Enginyeria Química i Química Analítica

Dr. José Luís Fernández Turiel
Institut de Ciències de la Terra Jaume Almera (ICTJA), CSIC

Grau de Química

Treball Final de Grau

Environmental impact of volcanic eruptions by experimental ash leaching.

Impacte ambiental d'erupcions volcàniques mitjançant la lixiviació experimental de cendres.

Judit Lloreda Rodes

January 2020

UNIVERSITAT DE BARCELONA

B:KC Barcelona Knowledge Campus
Campus d'Excel·lència Internacional

Volcanoes are in fact indexes of danger, and the absence of them is the best security.

James D. Dana

M'agradaria agrair al José Luís Fernández Turiel i a la Marta Rejas l'oportunitat de treballar amb ells, tota l'ajuda i els consells que m'han donat durant aquest mesos. Gràcies per fer-me sentir com a casa i per ajudar-me a descobrir un nou món. També donar les gracies a l'ITCJA i al CSIC per acollir-me aquest semestre. Agrair també al Fermín López tots les aportacions i el seu punt de vista a aquest treball. Gràcies a l'Andrea, la Maria i l'Anna per no perdre la paciència durant aquests quatre anys i mig d'aventura. I gràcies a la meva família, per estar-hi sempre i donar-me ànims per seguir endavant. Ara si avi, he acabat la carrera.

D'altra banda, donar les gràcies a Juan Pablo Carbonell i a Elisabeth Pintar per facilitar-nos les mostres de cendres de les excavacions arqueològiques de la Cueva Abra del Toro i de la Cueva de Salamanca a l'Argentina. El meu agraïment per l'assistència analítica dels Serveis de l'ICTJA-CSIC, Laboratori de Geoquímica labGEOTOP (infraestructura cofinançada per ERDF-EU Ref. CSIC08-4E-001) i de DRX (infraestructura cofinançada per ERDF-EU Ref. CSIC10-4E-141) (M. Rejas, J. Ibañez i S. Alvarez). Aquest treball ha estat parcialment finançat pels projectes ASH i QUECA (MINECO, CGL2008–00099 i CGL2011–23307) i el projecte LAJIAL (ref. PGC2018-101027-B-I00, MCIU/AEI/FEDER, EU). Aquest estudi s'ha realitzat en el marc dels grup de recerca consolidat GEOPAM (Generalitat de Catalunya, 2017 SGR 1494).

REPORT

CONTENTS

1. SUMMARY

Explosive volcanic eruptions eject large quantities of volcanic ash to the atmosphere. Much of these ash deposits on the ground and remains exposed to atmospheric conditions. During rainfall episodes or when ash falls on surface waters, they interact, easing the release of many elements into the environment. Reactive transport models, by leaching tests, allow experimental simulations of ash-water interactions, enabling to quantify the geochemical fluxes.

For this study, four ash samples from the Cerro Blanco eruption, in southern Puna (Argentina) were submitted to batch and column leaching tests. This eruption happened 4,200 years ago and it is one of the most important of the last 11,700 years (the Holocene) in the world. Two of the samples come from inside of two archaeological sites, believed by archaeologists to be inhabited until the eruption. After analysing the results of bulk composition and batch tests, anthropogenic contributions to one of them are proposed.

Both column and batch tests confirm the alteration of geochemical balance after rainfall episodes, causing stress for the environment. Results show the large number and quantities of elements that volcanic ashes can release, but also a general trend of low mobility. However, is noticeable the significant mobility and high concentrations in solution of potential toxic trace elements (PTTEs) like As, Sb and Cr.

The considerable release of nutrient as Na, Ca, K, Mg and P confirms the fertilizing potential of volcanic ashes. Furthermore, the release of PTTEs suppose environmental concerns to local ecosystems, even after thousands of years after the eruption. Results show that the geochemical hazard of volcanic ash can be assessed by leaching tests, being very useful for specific emergency response to volcanic eruptions.

Keywords: volcanic ash, volcanic eruption, batch leaching, column leaching, reactive transport models.

2. RESUM

Les erupcions volcàniques explosives expulsen a l'atmosfera grans quantitats de cendra volcànica. Bona part d'aquesta cendra es diposita a terra i queda exposada a les condicions atmosfèriques. Durant els episodis de pluges o quan les cendres cauen sobre aigües superficials, interactuen, facilitant l'alliberament de molts elements al medi. Els models de transport reactius, mitjançant proves de lixiviació, permeten realitzar simulacions experimentals d'interaccions cendra-aigua facilitant la quantificació de fluxos geoquímics.

Per a aquest estudi, quatre mostres de cendra de l'erupció de Cerro Blanco, al sud de la Puna (Argentina), es van sotmetre a proves de lixiviació en batch i en columna. Aquesta erupció es va produir fa 4,200 anys i és una de les més importants dels últims 11,700 anys (l'Holocè) del món. Dues de les mostres provenen de l'interior de dos jaciments arqueològics, dels quals els arqueòlegs creuen que va estar habitats fins abans de l'erupció. Després d'analitzar els resultats de composició total i dels batch, es proposen aportacions antropogèniques a una d'elles.

Tant les proves de columna com les de batch confirmen l'alteració de l'equilibri geoquímic després d'episodis de pluges, provocant estrès al medi. Els resultats mostren el gran número i quantitat d'elements que les cendres volcàniques poden alliberar, però també una tendència general de baixa mobilitat. Tot i això, destaca la gran mobilitat i altes concentracions en solució de possibles elements traça tòxics (PTTEs) com As, Sb i Cr.

El considerable alliberament de nutrients com Na, Ca, K, Mg i P confirma el potencial fertilitzant de les cendres volcàniques. A més, l'alliberament de PTTEs pressuposa preocupacions ambientals als ecosistemes locals, fins i tot milers d'anys després de l'erupció. Els resultats mostren que el perill geoquímic de la cendra volcànica pot ser avaluat mitjançant experiments de lixiviació, resultant molt útils per respostes específiques d'emergència enfront erupcions volcàniques.

Paraules clau: cendra volcànica, erupció volcànica, lixiviació en batch, lixiviació en columna, models de transport reactius.

3. INTRODUCTION

Gas, magma and solid fragments of rocks are expelled to the Earth's surface and atmosphere during volcanic eruptions. Any fragmented solid material ejected is called tephra[1]. Depending on its fragment size, tephra can be classified as: ash (less than <2 mm diameter), lapilli (2 mm to 64 mm) and blocks or bombs (larger than 64 mm). In an eruption column, smallest fragments of tephra, are dispersed in a gas phase (volcanic gases and air), arriving up to hundreds of thousands of kilometers from the source.

The consequences of an explosive volcanic eruption can be many and very varied, from complications in aviation, passing by health hazards to climate changes. This work will be focused on environmental impact of volcanic ashes from Cerro Blanco eruption, one of the largest explosive eruptions of Holocene[2]. Geochemical fluxes of the eruption over soil and water will be assessed, by batch and column leaching experiments, to quantify environmental concerns at regional scale.

3.1. EXPLOSIVE VOLCANISM

Volcanoes are the surface evidence of the internal dynamics of the Earth. Volcanic activity has modified the planet for thousands of millions of years, and it still happens nowadays. Effusive and explosive are the two most common types of eruption, showing each one opposite characteristics and properties (Figure 1). Every eruption is unique.

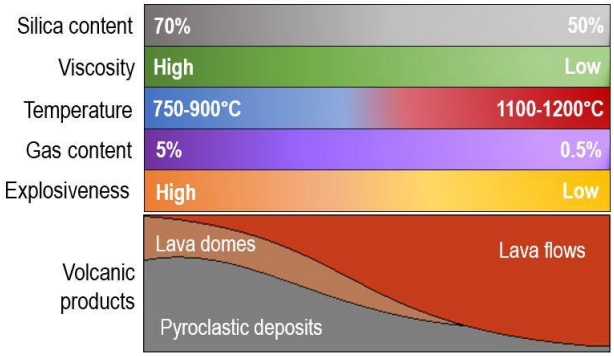

Fig. 1: Characteristics and volcanic products of explosive (left) and effusive (right) eruption types[1].

Rheological properties of magmas are conditioned by its chemical composition, pressure and temperature. The high content in silica (above 70%) increases significantly the viscosity of the magma, hindering the mobility and the degassing process. When pressure decreases abrupt degasification takes place, high viscous magma blows up instead of flowing, and an explosive eruption takes place, ejecting large quantities of tephra to the environment. Pyroclastic deposits and lava domes are common volcanic products of most explosive eruptions.

Wygel, C. M.; et. al. (2019)[3] suggested that rhyolitic eruptions, the ones with rich-silicic compositions and a large explosive behaviour, cause long-time exposure hazards in the affected region.

3.2. VOLCANIC ASH

Volcanic ash, whose composition is mostly glass (amorphous SiO_2), shows specific characteristics depending on the eruption type. As said previously, rhyolitic magmas blow up when volcano erupts. During high explosive eruptions ash particles undergo severe fragmentation, reducing their size and developing angular morphologies. Viscosity of magma largely determines the morphology of ash particles[4].

Furthermore, volatile components induce pre-eruptive vesicles in ash particles; as higher the volcanic explosive index (VEI) more bubbles inside ash fragments[3]. Irregular shape and fragmentation increases ash surface area, easing the coating with much smaller fragments on its surface. As more fine particulate matter on ash surface, greater will be the environmental available fraction of released elements to regional ecosystem. At the same time, particulate material is harmful at inhalation.

3.2.1. Ash particles – volcanic aerosols interactions

Reactions that take place in the eruptive plume between ash particles, volcanic gases and atmospheric aerosols remain poorly understood[5]. It is widely accepted that the fast release of several elements (major, minor and/or trace) during ash-water interaction is due to the presence of soluble salts in the surface of the ash particles[6,7]. Scanning Electron Microscope (SEM) images of many different ash samples confirms that the presence of smallest particles over glass surface may occur[4].

How these soluble salts deposit on the surface of ash particles is still unknown. Several studies have been and are being made in order to clarify the processes and mechanisms. The adsorption of volcanic salt aerosols on ash particles surface is the most accepted theory by scientific community. The ash-gas interaction in volcanic plumes is one of the main focus of research for volcanologists

and geochemists nowadays. Conclusive results of how the interaction occurs cannot be obtained from the current studies.

3.3. ENVIRONMENTAL IMPACT

During and after a volcanic eruption, the ejected volcanic ash becomes an agent that interacts with its surroundings, affecting ecosystems and inducing physical, biological and chemical effects in them. As Earth is an ensemble of interconnected ecosystems, knowing how ashes affect one of them is crucial to understand further consequences in the rest[8]. The treated below about environmental impact of volcanic ashes will refer to chemical impact on the hydrosphere.

When volcanic ashes are in the Critical Zone[9], i.e., in the dynamic interface between the soil and its fluid envelopes, some elements are leached, originating different geochemical fluxes. Depending on the climate of the region, the ash-water contact can take place in relative short times for humid climates, but could take long periods of time if the climate is arid.

These fluxes normally contain high concentrations of soluble elements as Na, K, Mg and Ca, but also traces of F, As, Sb, Cr, Pb, etc., that are potentially toxic trace elements (PTTEs). Some of these elements are micro and macronutrients that evidence the fertilizing power of volcanic ashes. However, and depending on their concentration, many trace elements (including micronutrients) represent a threat for health and must be monitored to prevent diseases. Trace elements toxicity is related to the solubility of their ions and/or complexes in water[10], and their bioaccumulation since they not degrade[3]. Even very low concentrations of them cause several disorders.

In any case, the release of so many elements from the ash to the environment have different consequences at regional scale, either beneficial or harmful. Those dragged elements normally end in surface and groundwater, and could be subsequently consumed by humans, animals and plants. Determine the amount of these PTTEs dragged to the aqueous environment is key to conclude the environmental impact of explosive volcanic eruptions into the Critical Zone. Thus, knowing the geochemical hazard of volcanic ashes is crucial for specific emergency response of volcanic crisis.

3.3.1. Reactive transport models

Any system, as volcanic ash in contact with water, involves a competition between reaction and transport. This ratio defines the principle of reactive transport models (RTMs)[11], commonly used in geosciences to understand and anticipate the migration of several elements and/or contaminants. For this study two RTMs will be considered: the batch and the flow-through models.

The batch model consists of a perfectly closed system, where chemical transformations are function of time, reaching an equilibrium state. This model fits with short-term effects and can be used as a first response measure just after an explosive eruption. Otherwise, the flow-through model consists of an open system where not only time but also transport determine chemical transformations. This model fits with long-term effects and is used to determine future release of compounds.

3.3.2. Short and long-term effects

Given the information provided by RTMs, short and long-term effects are similar but not the same. Both induce biogeochemical stress and significant changes on the geochemical balance of the region[12]. For example, producing changes in pH (normally increasing) in water systems due to dissolution of alkaline compounds and releasing hydroxyl groups from silicate minerals[13].

Short-term effects that take place just after the eruption are directly related to the release of water-soluble compounds, the most mobile ones, which are generally adsorbed onto the ash-particles surface during ash-water interaction.

Instead, long-term effects occur after the eruption. They are related to the weathering of volcanic ash constituents, glass and minerals, by hydrolysis, oxidation, dissolution and/or ionic exchange reactions[14].

3.4. GEOLOGICAL SETTING

The Cerro Blanco Volcanic Complex (CBVC) is located 3,500-4,700 m above sea level in southern Puna, NW Argentina. The complex is placed in San Buenaventura Cordillera, as part of the Andean Cordillera. The geographical location of CVBC is crucial to explain the characteristic volcanic activity of the region.

The subduction zone between Nazca Plate (oceanic plate) and South American plate (continental plate) causes an active continental margin, with associated volcanism, known as a Chile-type subduction zone[1]. The region is characterized by strong earthquakes and large explosive volcanos. The Andean Volcanic Arc is divided in four main volcanic zones, and Cerro Blanco is in the central one (CVZ) (Figure 2).

As the oceanic plate, cold and wet, goes downward the continental plate magmas are generated by partial melting. The increase of temperature and pressure dehydrate the subducted plate, releasing

aqueous fluids that decrease the melting point of silicate minerals[15]. These interactions give rise to a zone of partial melting in the continental plate.

Magma rising to the surface is difficult through continental plate, leading often to the formation of chambers where magma accumulates during large periods of time. The differentiation processes that take place during the storage could also generate more volatile compounds[1]. Some of the magmas evolve to rhyolitic compositions, with a high percentage of SiO_2 and being enriched in volatile components.

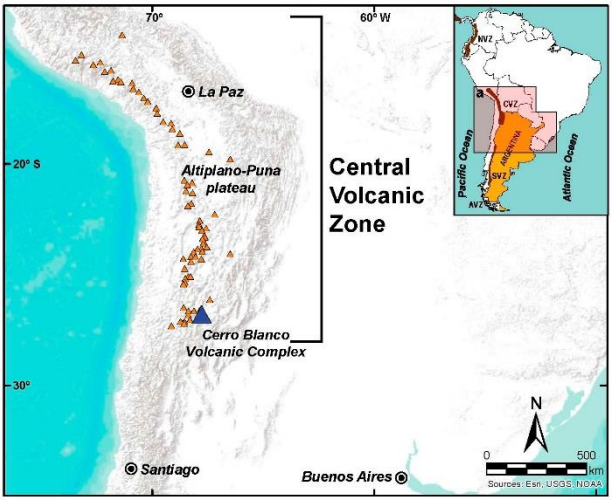

Fig. 2: Andean Central Volcanic Zone and Cerro Blanco Volcanic Complex location, remarked with a blue triangle. Orange triangles mark other Holocene volcanoes of the CVZ.
(figure adapted from Fernandez-Turiel, J. L.; et. al. (2019), ref. 2)

The material ejected, the column eruption height and the duration of the explosion define the Volcanic Explosive Index of an eruption. With a VEI of 7, Cerro Blanco eruption is considered one of the largest eruptions of the Holocene, from 4,410–4,150 cal BP (calibrated years before present). With more than 100km^3 of tephra were ejected, Fernandez-Turiel, J. L.; et. al. (2019)[2] estimate a dens-rock equivalent volume (V_{DRE}) of 75 km^3 for a dens-rock density (ρ_{DRE}) of 2,300 kg/m^3.

Chemical and mineralogical composition of Cerro Blanco caldera was also characterized by Fernandez-Turiel, J. L. and co-workers in previous studies[2]. Rhyolitic glass (75-80% SiO_2) is the most abundant phase, with presence of K-feldspars, quartz and biotite. Fe-Ti oxides (with Mn oxide) are also present as minor phases. The rhyolitic composition gives the ash a whitish colouring.

3.5. BACKGROUND OF ANALYTICAL METHODS AND TECHNIQUES

For ash studies, either volcanic or environmental, several techniques can be used. The results obtained by various techniques and methods are interpreted together to obtain a general comprehension of ash properties and characteristics. Depending on the characterization performed, methods and techniques can be grouped in physical, mineralogical or chemical categories.

Physical characterization comprehends techniques like SEM for morphology information, Brunauer-Emmett-Teller (BET) analysis for texture and specific surface area, and laser diffraction (LD) for grain size distribution.

Chemical characterization techniques comprehend the analysis of the whole rock by Inductively Coupled Plasma Spectrometry (ICP), either ICP-AES (atomic emission) or ICP-MS (mass spectrometry), and X-ray fluorescence spectrometry (XRF). X-ray diffraction (XRD) allows to know the mineralogical composition of the ash. Used for quantitative micro-chemical characterization[16], Electron probe micro-analyzer (EPMA) and Laser Ablation coupled to ICP-MS (LA-ICP-MS) give accurate results.

There is no standard method for volcanic ash leachates analysis. Through years several research groups have develop their own protocols. Although, the methods and techniques used have been mostly the same and have improved over the years. Witham, C. S.; et. al. (2005)[6] gathered information about volcanic ash leachates analysis, the purpose of the study, and the techniques and methods used in several previous works.

For majority of elements, specially metals, Atomic Absorption Spectrometry (AAS) was replaced by ICP-AES or ICP-MS. Lately, ICP-MS become largely used due to its high sensibility and multi-element capacity for analysis. Ion chromatography is used to measure anions (like Cl^- or SO_4^{2-}), and ion-selective electrode (ISE) potentiometry for fluoride determination. These two methods are still largely used, since there are no better techniques that can replace them.

4. OBJECTIVES

The main objective of this study is to understand the geochemical hazard of volcanic ashes in order to develop specific emergency responses for volcanic crisis. Several features of volcanic ash-water interactions will be assessed by two reactive transport models, taking on reference the case study of the large 4.2 ka eruption of Cerro Blanco, in Central Andes.

More specific objectives are:

- ✓ Compare batch and flow-through leaching tests as tools for reactive transport modeling.
- ✓ Identify and quantify the geochemical fluxes to the Critical Zone.
- ✓ Assess possible chemical benefits and/or threads of volcanic ash in environment.

5. METHODS

5.1. SAMPLING

Studied ash samples of Cerro Blanco eruption come from two archaeological sites in rocky shelters. Samples collected from inside these sites were M-508 from Salamanca Cave 1 in the Puna (geographical coordinates, datum WGS84, 26° 01' 18.11" S and 67° 20' 31.57" W, 3,665 m a.s.l.)[17], and "Muestra 10" from Abra del Toro cave in Yocavil valley (26° 58' 07.30" S and 66° 00' 27.30" W, 2,966 m a.s.l.).

In addition, two samples from outside geological outcrops archaeological sites were collected to compare internal and external behaviors. AS-04 in the Puna (26° 18' 49.78" S and 67° 23' 53.69" W, 3,148 m a.s.l.) and "Ceniza Talud" in Yocavil valley (26° 58' 07.82" S and 66° 00' 24.25" W, 2,982 m a.s.l.) The names assigned by archaeologists to each ash sample have been respected for this study in order to avoid confusions in future reports.

5.2. PHYSICAL AND MINERALOGICAL CHARACTERIZATION

Physical characterization was made by a FEI Quanta 200 ESEM FEG Scanning Electron Microscope (SEM) equipped with an Energy Dispersive X-ray system (EDX). Ash samples were mounted on carbon stubs and coated with carbon before being examined at different magnifications for morphological features, and later analyzed by EDX for a semi-quantitative chemical analysis.

Mineralogical characterization was made by X-ray diffraction (XRD) analysis. Samples were powdered in an agate mortar and the diffractograms were obtained using a Bruker D8-A25 instrument (Cu K-α1 radiation, λ=1.5406 Å, at 40 kV and 40 mA), collecting data between 4° and 60° of 2θ, with a scan step of 0.035° and an equivalent step time of 384 s. Diffractogram evaluations were carried out using the DIFFRAC software.

5.3. BULK CHEMICAL ANALYSIS

The bulk chemical analysis for all samples was carried out by High Resolution-Inductively Coupled Plasma-Mass Spectrometry (HR-ICP-MS, Element XR, Thermo Scientific). Major, minor and trace elements were determined simultaneously. For each sample, 0.1 g were digested with HNO_3:$HClO_4$:HF (2.5:2.5:5 mL, v/v), doubly evaporated to incipient dryness with addition of HNO_3, and finally made up to 100 mL with 1% (v/v) HNO_3[12,13]. Loss on ignition (LOI) was determined on 0.5 g of sample at 1000°C.

5.4. ASH LEACHING TESTS

Batch experiments in triplicate were carried out for all samples. One gram of ash was mixed with 10 mL of Milli-Q Plus ultrapure water type (18.2 MΩ·cm) in 14 x 100 mm polypropylene (PP) test tubes. Water leachates were shaken for 4 hours at 20 rpm and subsequently filtered through polyvinylidene difluoride (PVDF) syringe filters with tube tips (Whatman, 25 mm diameter and 0.45 µm pore size)[18]. Finally added 1% (v/v) HNO_3 up to 100 mL.

Specific Conductivity (SC) and pH were monitored by means of specific electrodes (Crison Multimeter MM40) immediately after mixing the ash and the deionized water (pH_o and SC_o), and after shaking (pH_f and SC_f), prior to filtering. Major and trace elements were determined by HR-ICP-MS.

Flow-through column test were carried out for samples AS-04 and “Muestra 10”: ten grams of ash were filled in an 8 cm long and 2.25 cm^2 cross-sectional-area cartridge (Teledyne ISCO). Cartridge

loading was carried out gradually in order to avoid the development of air bubbles, and a silica filter (60 Å average pore size diameter) was attached at the cartridge inlet and outlet.

A peristaltic pump (Gilson Minipuls 3, operating at 15 rpm) at the head of the column ensured a constant and stable deionized flow of water (Milli-Q Plus type, 18.2 MΩ·cm) with an average discharge of 0.12 mL/min. A fraction collector (Gilson FC 204) at the column outlet stored samples from the leaching solution into 14 x 100 mm PP test tubes (400 drops/tube).

For AS-04 a percolated solution of 687 mL was collected in 5 days, resulting in a set of 92 tube samples; a subset of 30 tubes was analyzed for major and trace elements by HR-ICP-MS. For "Muestra 10", a percolated solution of 676mL was also collected in 5 days, resulting in a set of 67 tube samples; a subset of 20 tubes was analyzed by HR-ICP-MS.

In both tests, all tube samples were weighed and analyzed for pH and SC (Crison Multimeter MM40) immediately after tube filling and acidified by addition of 1 drop of HNO_3 to each tube. Finally stored at 4°C until analysis.

5.5. DATA PRESENTATION

X-ray diffractogram and general SEM images of the studied samples are shown on Appendix 1. Major oxide contents of bulk chemical analysis are shown in Table 1, also with LOI values. For batch experiments, pH, SC and total concentration of dissolved ions are shown on Table 2. Trends of SC and pH for column tests are on Figure 3.

Element mobility and environmental contribution are expressed as relative mass leached (RML) and total contribution (TC), respectively. The TC of an eruption to the geochemical balance of a region[13] is calculated for each element as the product of the RML by the eruption mass (M). For the Cerro Blanco eruption M is 1.725×10^{11} Mg, and is calculated as the product of the volume of dens-rock equivalent (V_{DRE}) by the density of dens-rock equivalent (ρ_{DRE}). These estimates correspond to non-pristine ashes, i.e., were exposed to climate conditions during about 4,200 years. Consequently, the results are minimal estimates.

RML represent the percentage of an element that can be mobilized through ash-water interaction[18], and is calculated as the fraction between the element concentration in the leachates over the element concentration in the bulk in percent. Depending on its value, elements were arbitrarily grouped in: mobile (RML higher than 1%), moderately mobile (between 1% and 0.5%), low mobile (between 0.5% and 0.01%) and extremely low mobile elements (less than 0.01%).

Relative mass leached and total contribution values for batch and column tests are shown on Appendixes 2 and 3, respectively. For column tests, elements behaviour as function of time are shown on trend graphics in Figures 4 and 5 for sample “Muestra 10”, and Figures 6 and 7 for sample AS-04.

6. RESULTS AND DISCUSSION

6.1 ASH CHARACTERIZATION

XRD diffractograms of the four samples (Appendix 1, Fig. A1.1) are almost identical between them. As every eruption is compositionally unique, it can be proved that all analysed ashes belong to the same volcanic eruption, the Cerro Blanco eruption.

The curvilinear baseline of the diffraction patterns indicates the presence of amorphous material in the samples, which corresponds to volcanic glass (amorphous SiO_2). Quartz (crystalline SiO_2), sanidine (potassium feldspars), andesine (plagioclase) and biotite minerals were also characterized. Mineralogical composition is coherent with previous studies[2].

EDX spectrums confirms the presence of glass in all samples, showing peaks for Si, K, and Al with different Si:K ratios. K-feldspar (Si, K and Al), plagioclase (Si, Al, Ca and K) and biotite (Si, K, Fe and Al) were identify too. Additionally, Fe-Ti oxides with manganese and pyrite were also detected with the dual back-scattered detector (DualBSD). Exceptionally, metallic silver was found on sample “Muestra 10”.

SEM images (Appendix 1, Fig. A1.2) show a very fragmented material with angular shapes, consistent with ash from explosive eruptions[4]. In AS-04 and “Ceniza Talud” samples (from outside archaeological sites) can be appreciated grains with much smaller size deposited on biggest fragments surface, giving them a brighter coloration. Instead, in samples M-508 and “Muestra 10” (from inside) this covering of smaller particulate matter is barely appreciated resulting in a darker coloration.

Coating is a bit higher in M-508 than in “Muestra 10”, but in any case, smaller than in outside samples. The transport process, mainly due to wind, from outside to inside the archaeological sites may be the explanation to this apparent lack of small particulate matter on ash particles surface. Wind

should have deposited the biggest ash fragments, carrying away the smallest ones during the process.

6.2. ASH COMPOSITION

Whole-rock chemical analysis accentuates the similar compositions of the four ashes, and trends between samples from same archaeological sites (Table 1). Silica content (>75%), as well as Na, K and Ca oxides concentration are coherent with previous studies[2]. Loss of ignition results (>1%) confirm the high presence of volatile components in the ash samples. Volatile weathering products, such as water, also contribute to LOI percentage; being it the most probable explanation for those raised values, higher than 2% for all samples.

Table 1: Major oxides concentration and LOI, both in mass percentage, for each ash sample.

Major oxides	AS-04 [% m/m]	M-508 [% m/m]	Ceniza Talud [% m/m]	Muestra 10 [% m/m]
SiO_2	77.86	77.70	76.07	76.80
Al_2O_3	11.21	10.97	11.82	11.16
Fe_2O_3	0.51	1.23	0.83	0.62
MnO	0.06	0.05	0.06	0.06
MgO	<LoD	0.28	0.24	0.15
CaO	0.66	1.16	0.66	0.60
Na_2O	2.92	2.83	2.96	2.67
K_2O	3.72	2.99	3.57	3.96
TiO_2	0.09	0.32	0.16	0.12
P_2O_5	0.01	0.04	0.03	0.02
LOI	2.95	2.45	3.61	3.83

A deeper analysis of trace elements concentration exposed singular differences between sample M-508 and the other: exceptionally higher values for Sr, Ba and V, as well as remarkable concentrations of Cr and Ni. Although it was not detected by XRD, the presence of small portions of gypsum ($CaSO_4 \cdot 2H_2O$) could explain the high values of Sr in the sample.

6.3. BATCH LEACHING EXPERIMENTS

The batch experiments suggest similar trends between samples, however sample M-508 outline, not because of its behaviour but because of the differences in the general characteristics of pH and SC regarding the other three.

6.3.1. Specific conductivity and pH

Just after ash-water interaction, batch leachates show slightly alkaline pH and low values of specific conductivity (Table 2). Samples AS-04, "Ceniza Talud" and "Muestra 10" show an initial pH range of 8.8 – 7.8, quite similar to after ash-water interaction values. After 4h of shaking, SC increases in all samples. It is the expected behaviour as many ions, especially most soluble compounds, are released to water leachates during interaction.

Table 2: pH and specific conductivity values, before and after shaking, and total concentration of dissolved ions from batch tests, of three replicates for each sample.

Sample	pH_o	pH_f	SC_o [µS/cm]	SC_f [µS/cm]	Total ions [mg/L]
AS-04	8.34	8.12	19.90	51.00	96.58
	8.22	8.28	10.08	39.80	96.10
	8.02	8.10	10.97	41.30	95.18
M-508	7.18	7.24	620.00	983.00	366.17
	7.03	6.57	228.00	920.00	324.09
	6.85	6.63	430.00	895.00	330.71
Ceniza Talud	8.79	8.80	25.70	40.20	93.20
	8.39	8.64	22.72	49.00	93.08
	8.60	8.76	18.71	41.50	93.13
Muestra 10	8.64	8.53	7.71	16.45	85.20
	8.37	8.27	6.54	18.35	85.89
	7.81	7.99	11.90	22.10	86.41

The reaction of silicate minerals with water explains the basic pH values measured. When water molecules contact with terminal and superficial oxo-groups, a dissociative chemisorption takes place[19]. Through this process, a proton from the water molecule is retained in silicate structure and a hydroxyl ion is released into the dissolution. Moreover, the dissolution and ionic exchange of alkaline compounds by protons[12] also contributes to basic pH. In further stages of dissolution, an equilibrium is reached leading to neutral values of pH.

However, sample M-508 shows neutral or slightly acidic pH values and a SC of an order of magnitude higher, both initial and final values. Total concentration of dissolved ions is also noticeable. Small particulate matter on ash surface cannot be a significant explanation, as both inside samples are similar between them and different from the outside ones.

Due to its location inside the inhabited archaeological site[17], close to the surface level of excavation, anthropogenic contributions are suggested. Human activity in the cave may have altered its composition, being the reason for the different pH and SC values.

6.3.2. Leachate composition

In general terms, all leachates have the same composition, showing a similar behaviour when interacts with water. Around 30-35 elements were detected for sample (Appendix 2, Tables A2.1 and A2.2). Highest concentrations were given for Na, Ca, K, Cl and S (>1 mg/kg); Mg, Si and Fe are also present in major concentrations. Elements V, Ga, Mo, Cd, Cs, Hg and REE were not detected, except for La, Ce and Nd. It is also remarkable the presence of trace elements As, Sb, Cr and Pb as PTTEs.

Sample M-508 outlines again. Up to 41 elements were detected by HR-ICP-MS analysis showing, for majority of elements detected, highest concentrations respect the other three samples. In some cases, like for Ca, Mg, Na, Cl, B, Mn, Sr and Ba, raised an order of magnitude.

Aluminium concentration in sample AS-04 is higher than for the other samples. This indicates that cation Al^{3+} is part of a more soluble mineral, probably due to weathering reactions. Changes in ion concentration in water leachates may be due to weathering processes that generate more soluble compounds.

Another different behaviour can be observed in La and Ce. For sample AS-04 La concentration is higher than Ce concentration, and vice versa for samples M-508 and “Muestra 10”. Also, concentrations for AS-04 are one order of magnitude higher. These results could be due to the nugget effect.

The nugget effect describes the heterogeneity between different samples, according to geological and sampling components[20]. Sampling effects are not considered in this work because of the small grain size of the particles of the sample (<200 nm). Geological effects are related to the natural distribution of elements and cannot be removed. The high contents of La and Ce in AS-04, together with the high content of P suggest the occurrence of apatite. This calcium phosphate mineral often contains high concentrations of the cited elements.

Reproducibility diagrams were plot for reproducibility analysis. Although in general the deviation of the replicates is low or very low for majority of elements, for others (like La, Ce and Ni) is considerably high. This is probably a result of the before mentioned nugget effect. Sample AS-04 is the one that presents more elements with high deviations. It is recommended to perform at least three replicates for batch tests to obtain reproducible results.

6.3.3. Element mobility

For batch tests there are no elements with an RML>1%. It is reasonable if it is considered that samples come from a 4,200 years old eruption, and that have been exposed to the local climatic conditions during all this time. Despite that, a general categorization of elements could be:

- Moderately mobile elements: Sn and Ni (just for sample AS-04).
- Low mobile elements: Ca, Mg, P, Cr, Ni, Cu, Zn, As (except for "Muestra 10"), Sr, Sb and Fe (except for M-508). As well Na, K, Mn, Li and Hf in M-508; Sc, Ba, La and Ce in AS-04; and Na in "Ceniza Talud".
- Extremely low mobile elements: Na, K, Si, Ti, Al, Mn, Li, Be, Rb, Zr, Ba, La, Ce, Nd, Hf and Pb. Also, Th and U in M-508.

Apart from the general low mobility trend observed in batch tests, it is remarkable the low or even extremely low mobility of major elements, like Na, K and Ca. Although their concentrations in solution are high, the portions that have been removed from ashes are low. Mobility for As, Sb, and Cr indicate that these PTTEs are more soluble that other elements considered nutrients.

Most mobile element is Sn (RML of 0.6-0.7%), probably because is part of a high soluble compound. Nickel, with an RML of 0.8% in sample AS-04, must also be part of a high soluble compound.

6.4. COLUMN LEACHING EXPERIMENTS

Column leaching tests, with a continuous flow of water, allow to characterize when elements are released to solution, as well as group them depending on their trends. The two tests performed with inside and outside samples confirm the differences between them, especially when it refers to specific conductivity.

6.4.1. Specific conductivity and pH

First value of SC in the sample sequence is the highest one, as smallest grain sizes are released. Maximums were 43 µS/cm for sample "Muestra 10" and 390 µS/cm for AS-04. Here it can be observed the main difference between the two ashes. The total amount of ions dissolved for the outside sample is much higher than for the inside one. These results were expected as smaller particulate matter for "Muestra 10" is less than for sample AS-04.

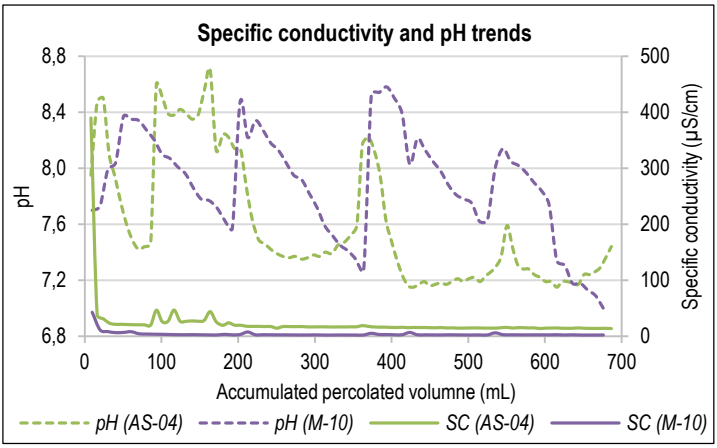

Fig. 3: Specific conductivity and pH values plot in front the accumulated percolated volume. Green color for sample AS-04 and purple for sample "Muestra 10" (express like M-10). Dashed line for pH trend and continuous line for SC trend.

Progressively the SC decreases, very fast at the beginning and then slowly until it becomes constant. The average values at this point are 15 µS/cm for AS-04 and 2 µS/cm for "Muestra 10". Anyhow, there are some SC peaks that stand out from the constant values. These coincide with maximums (absolutes or relatives) in pH.

The obtained pH values shape an irregular trend, with several peaks. Both ashes show a slightly alkaline-neutral interval of pH: [8.6 – 7.0] for "Muestra 10" and [8.7 – 7.1] for AS-04. Basic pH match with firsts stages of silicate minerals dissolution, as well as the more neutral values with equilibrium processes. Basic peaks in the pattern suggest that dissolution of a mineral has taken place.

The patterns for both samples are different (Figure 3). AS-04 ash present more wide peaks, instead "Muestra 10" present a regular shape. In this sample, the pH oscillations vary following the same trend: maximum (basic pH), lineal decrease until a minimum, and then a maximum again. It is believed that the extremely low SC values (<5 µS/cm) caused error in the measure, as every maximum (except for the first one) match with different series of measures.

6.4.2. Leachate composition of sample "Muestra 10"

Up to 58 elements were detected, being Cd, Hg, Eu and Lu undetected. Highest element concentrations were given for Na, K, Ca, Si, Cl, Al and Fe. For each element, maximum concentration agrees with first value, except for nickel. Relative and/or absolute concentration peaks match with SC peaks, and with basic pH values.

A subset of 25 elements, the ones detected in all analyzed tubes and with concentrations higher than the limit of detection (LoD), were plot in order to set up trends between them. Those elements were grouped in four trends: sulphur, chlorine, silicon and aluminium (Figures 4-5). The chosen elements to name the groups represent the most significant element of the trend. The similarities on the shape of its outline was the criteria to group elements, attempting to coincide as many peaks as possible.

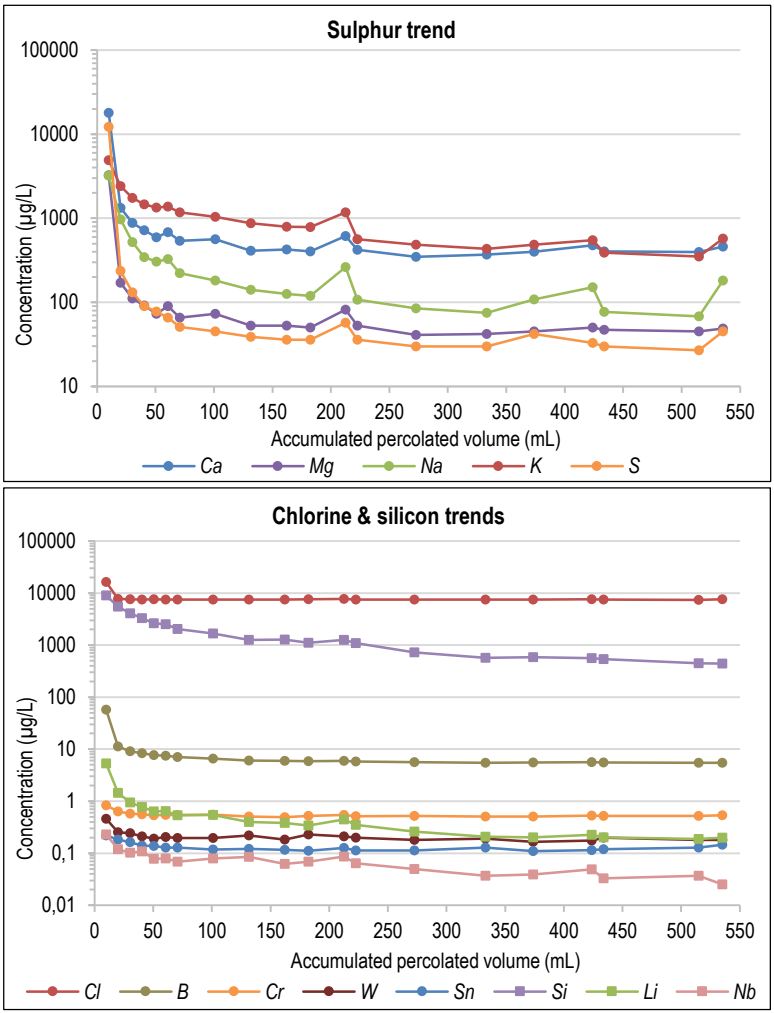

Fig. 4: Element concentration -vs- accumulated percolated volume graphics for sample "Muestra 10"; elements grouped in trends following similar behavior between them. Two different trends represented in the lower graphic (dots for chlorine trend and squares for silicon trend).

Sulphur, chlorine and silicon trends (Figure 4) present a constant behavior after an initial decrease in concentration. Sulphur trend present a huge initial decrease and a final slightly increase; also, a characteristic peak around 210 mL is appreciated. Chlorine and silicon ones do not present any significant peak; however, silicon trend shows more negative slope.

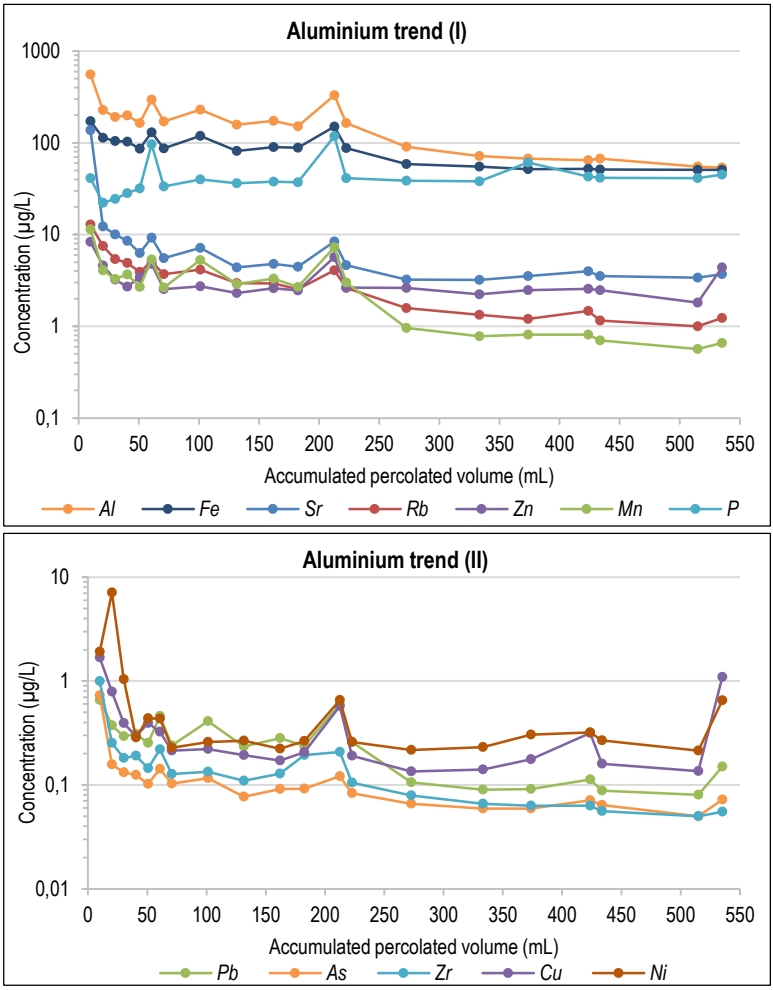

Fig. 5: Element concentration -vs- accumulated percolated volume graphics for sample "Muestra 10"; elements grouped in trends following similar behavior between them. The two graphics represent the same trend at different concentration scales, for better appreciation.

Aluminium trend (Figure 5) looks like sulphur trend, showing the same peak at 210 mL. The main difference, and characteristic, is the peak at 60 mL. Forming part of this trend are elements whose outlines are slightly different, being nickel and phosphorous the clearest examples.

All those outlines are coherent with an incongruent dissolution process, characteristic of aluminosilicates dissolution, where completely dissolution take several intermediate steps (normally formation of clays).

The elemental compositions of each trend is as follows:

- Sulphur trend: Ca, Mg, Na, K and S.
- Chlorine trend: Cl, B, Cr, W and Sn.
- Silicon trend: Si, Li and Nb.
- Aluminium trend: Al, Fe, Sr, Rb, Zn, Mn, P, Pb, As, Zr, Cu and Ni.

Those groups represent similar behaviour, suggesting that are part of the same type of compounds (glass or mineral). It is appreciated that most soluble cations are grouped with sulphur, likely occurring as sulphate, also a soluble anion. Transition metals, usually part of aluminosilicate structures, follow aluminium behaviour. Some REE and Y can also be grouped as part of the aluminium trend, but with more prominent peaks on its outline.

Resemblances between outlines, with same characteristic peaks in different trends, are not unexpected. As elements can be part of different compounds simultaneously, those similarities are normal. On contact with water, ionic exchange, dissolution and hydrolysis reactions take place. These weathering processes occur at different time, releasing different ions into the solution. The two first take place at low percolated volumes, as are fast processes. At higher percolated volumes, hydrolysis becomes predominant.

6.4.3. Leachate composition of sample AS-04

Again 58 elements were detected, being Cd, Tm, Eu and Lu undetected. Highest element concentrations were given for Al, Fe, P and Sr. For each element, major concentration match with first value, except for Al and P. Relative and/or absolute concentration peaks match with SC peaks, and with basic pH values.

This outside sample has a total ion concentration of flow-through experiment three times higher than inside sample. These results are coherent with SC values. The same 25 elements plot for sample “Muestra 10” trends were grouped for this sample, following the same criteria.

The grouping of elements for sample AS-04 was not as easy as for "Muestra 10". Some elements, especially transition metals, present cross outlines with characteristics from one and another. Similarities between elements from different trends are easily observed. To facilitate the classification, the same trends (sulphur, chlorine, silicon and aluminium) were assumed (Figures 6-7). Other classifications are possible, apart from the one presented here.

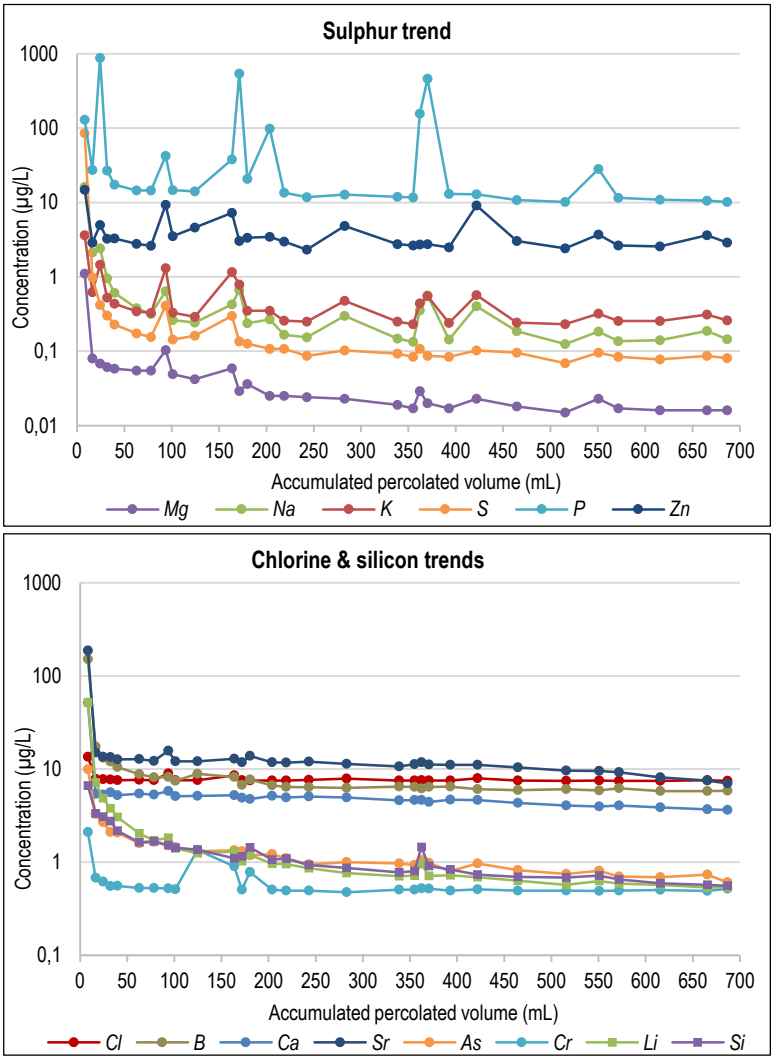

Fig. 6: Element concentration -vs- accumulated percolated volume graphics for sample AS-04; elements grouped in trends following similar behavior between them. Two different trends represented in the lower graphic (dots for chlorine trend and squares for silicon trend).

A remarkable difference is that, although both ashes come from the same eruption, the AS-04 sample contains smaller particulate matter (as seen in SEM images; Appendix 1, Fig. A1.2). This must be considered in all this chapter.

Sulphur, chlorine and silicon trends (Figure 6) are not as similar. Sulphur group present four characteristic concentration peaks (at 90 mL, 170 mL, 370 mL and 550 mL), with more peaks that are not shared for every element. Phosphorous outlines for peak's height, and zinc for not exhibiting one of the characteristic peaks.

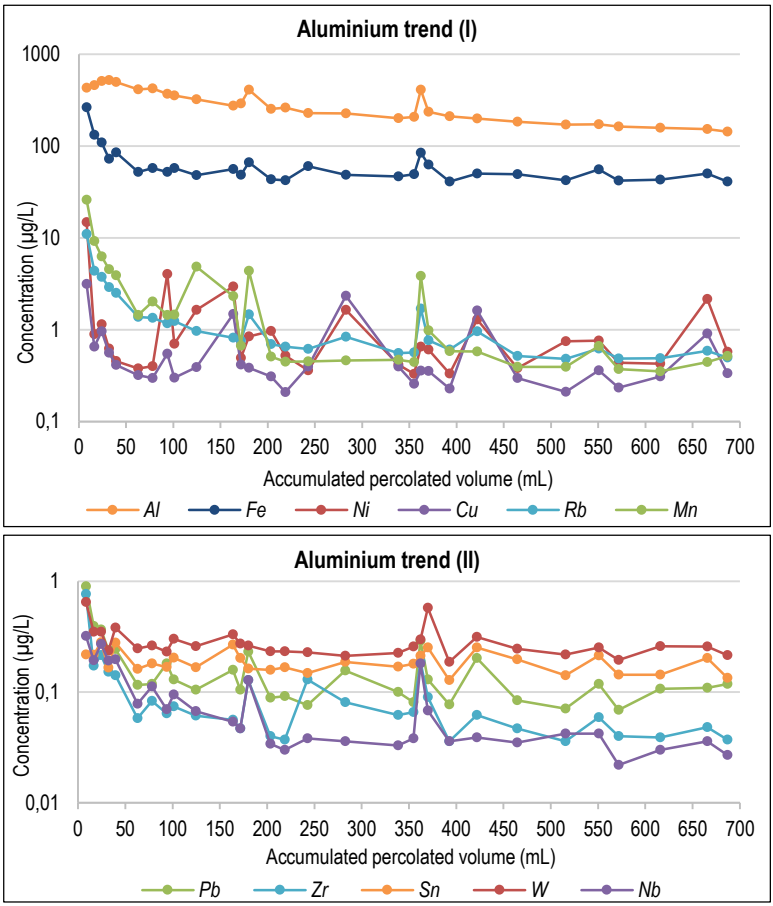

Fig. 7: Element concentration -vs- accumulated percolated volume graphics for sample AS-04; elements grouped in trends following similar behavior between them. The two graphics represent the same trend at different concentration scales, for better appreciation.

Chlorine and silicon trends are also quite similar, with an initial decrease in concentration and a further constant value. Some elements of the chlorine group show a very slightly peak at 90 mL, and silicon and lithium a peak at 37 0mL. Chromium is the irregular element, with a wide peak between 120-160 mL.

Aluminium trend (Figure 7) is the one that present more differences. Elements Al, Fe and Rb have the more similar outlines, that are at the same time very similar to the silicon trend. It is not surprising as Si, Al and Fe (in some cases) are the main components of aluminosilicates. However, a not so constant outline and the concentration peak at 180 mL difference them. Likewise, Al presents another significant difference at low percolated volumes: its concentration increases.

Transition metals of this group present irregular outlines, being the ones in the below graphic the most similar between them. All those elements have two peaks at 180 mL and 360 mL, coinciding so with aluminium. Manganese has the same wide peak as chromium, and nickel again showing a slightly different behaviour.

The elemental compositions of each trend is as follows:

- Sulphur trend: Mg, Na, K, P, Zn and S.
- Chlorine trend: Cl, B, Ca, Sr, As and Cr.
- Silicon trend: Si and Li.
- Aluminium trend: Al, Fe, Ni, Cu, Rb, Mn, Pb, Zr, Sn, W and Nb

Up to 8 elements are in different trends for both samples, being Ca and P the most remarkable. These changes in the behavior suggests that those elements are part of different compounds.

Must be remembered that outside sample was more exposed to climate conditions. Although the arid climate, sporadic rainfall episodes take place occasionally. Rainwater accelerate or facilitate weathering reactions, leading to more weathering products than for samples protected from meteorological conditions.

Oxidation reactions can also take place during weathering processes. A change in ions' oxidation state alter key properties like solubility or complexation. This result in different preferences in elements to combine with. Some non-coincidental peaks between elements and trend element (like Mn with Al), may have an explanation on ion's different oxidation states and the subsequent compound that is part of.

Rare earth elements and yttrium were not grouped as its concentration values were close or below LoD. Heaviest of these elements can be accommodated into common minerals, by substituting Al^{3+} cation[21]. It is not strange that they remain in the silicate structure, even after several weathering processes.

6.4.4. Element mobility

Although the longer time of ash-water interaction, for column test there are just mobile and moderately mobile elements (RML>1%) for sample AS-04. Highest values of RML are given for this sample; coherent result as three times more ions were released to water leachates. A general categorization of elements could be (Appendix 3, Table A3.1):

- Mobile elements: Sb (only for AS-04).
- Moderately mobile elements: Ca, P, Ni and Sr (only for AS-04)
- Low mobile elements: K, Fe, V, Cr, Cu, Zn, As, Sn and Ba; only for AS-04 also Na, Li and Co, for "Muestra 10" also Ca, P, Sr and Sb.
- Extremely low mobile elements: Si, Ti, Al, Be, Sc, Ga, Ge, Rb, Zr, Cs, Pb, Th, U, Y and REE; only for "Muestra 10" also Na, Li and Co

Although few elements present more mobile or moderately mobile RML coefficients, most elements still show a low or extremely low mobility. Major components, as Na, K, Si, Ti and Fe present a low or very low mobility, although they have a significant concentration in water leachates.

Surprisingly Sb is the most mobile element of outside sample (RML of 1.3%), followed by Ca, P and Ni. For inside sample phosphorous is the most mobile (RML of 0.3%), followed by Ni, Sr and Cr. Magnesium mobility is not calculated for AS-04 as its bulk composition is below LoD.

It is remarkable the high mobility of some PTTEs like As, Sb and Cr. In the same way, the mobility of micro-nutrients like Ni, Cu and Zn may become worrisome, as if high concentrations are released to the environment, they become toxic instead of beneficial. As indicate for batch tests, element mobility can be high even if concentration in water leachate is low.

6.5. COMPARISON BETWEEN BATCH AND COLUMN EXPERIMENTS

The differences between ash-water interaction and contact time produce similar but different results for the experiments. The simulation of two reactive transport models (RTM), which are related to migration of ions, show the main difference in RMLs data.

For batch experiments, simile of a closed system for the study of short-time effects, RML values are lower than for column experiments, a flow-through open system for long-time effects. In general, mobility coefficients slightly increase for all elements, even so remaining in the same category. Although, for others elements RML value decrease, as for Sn.

In batch experiments, less elements have concentrations that are above LoD. However, all elements detected in those experiments are also detected in column leachates, normally with higher concentrations. Also, element concentration in column tests are raised respect the batch tests.

Flow-through experiments let to describe the behaviour of ashes after rainfall episodes through long periods of time. Also allow to differentiate ashes with different grain sizes. For samples from the same eruption, batch results are quite similar, as expected. But column results, especially for elements behaviour, allow to clearly differentiate them. For the study case, with samples from outside and inside archaeological sites, SC values also confirm the differences in the quantity of ash smallest grain size.

6.6. GEOCHEMICAL CONTRIBUTION TO THE REGIONAL BALANCE

Values of total contribution give an idea about the quantity of elements released during ash-water interaction. The geochemical fluxes generated impact on the Critical Zone, for better and for worse. Knowing the approximate amount dragged is crucial to discuss environmental concerns on the region, and consequently specific emergency response to volcanic eruptions.

Cerro Blanco eruption highly affected the regional balance of the zone, by releasing large amounts to surface and groundwater. First, it will be analysed short time effects, the ones that should be considered just after the eruption. Although the eruption took place very long time ago, an approximation can be done with batch results (Appendix 2, Tables A2.1 and A2.2). Due to the time passed, the results obtain will be decreased.

Volcanic ashes could have transferred more than $1x10^8$ Mg of some elements to the local environment. Calcium and phosphorous are above this mass. Between $1x10^8$ Mg and $1x10^7$ Mg are elements as Na, Mg and K; and below $1x10^7$ Mg are Ti, Sn and Mn. Trace elements, silicon and aluminium contribute with less than $1x10^6$ Mg. Those quantities are estimates of what could had been released after the eruption.

Total contribution values from column experiments (Appendix 3, Table A3.1) are raised, respect the batch tests. This confirm that the potential of volcanic ashes to release elements long after the eruption is high, becoming a real hazard for nowadays.

Highest quantities are given for sample AS-04, with Ca and P a contribution above $1x10^9$ Mg. It is also noticeable Ni and Sb contributions, between $1x10^7$ Mg and $1x10^6$ Mg. For "Muestra 10" major contributions are also given for P, Ca and Mg (~$1x10^8$ Mg). Other sizeable contributions for both samples are: Na, K and Fe between $1x10^8$ Mg and $1x10^7$ Mg, and Si, Ti, Al and Mn between $1x10^7$ Mg and $1x10^6$ Mg. Trace elements Cr, Cu, Ni, Zn, As, Sr, Sn and Sb contribute with $1x10^5$ Mg.

Although every eruption is compositionally unique, eruptions from same volcanic region could unveil similarities in several characteristics. Total contribution from Cerro Blanco eruption was compared with another rhyolitic eruption from the same geographical zone. The 2008 eruption of Chaitén volcano, in Southern Chile.

The Chaitén eruption[13], smaller in magnitude and much closest in time, maximum contribution was between $1x10^5$ Mg and $1x10^4$ Mg. Listed in descending order, major concentrations were given for Ca, Na, Si, K, Mg, Al, As and Pb.

Comparing compositions from both eruptions, Cerro Blanco eruption show less concentrations for major oxides, except for Si and Mg, and LOI values are doubled. Trace elements as Sb, As and Cr present also reduced concentrations. Instead, for Ni is much higher. Considering the weathering reactions undergone by the ancient eruption and the huge magnitude of it, those changes in total contribution values are coherent.

Element mobility for batch tests is higher for Chaitén samples, but general categorization (considering the changes in magnitudes) of element done for the ancient eruption will also fit for it. Anyway, both eruptions follow the trend of general low mobility. In column experiments, elements behaviour is more disparate. It is noticeable that aluminium shows the same increase in concentration at the first stages of leaching, like in sample AS-04.

Additionally, a theoretical model of precipitation was developed in order to describe qualitatively the contribution to geochemical balance 4,200 years ago. Explanation of the model is shown on Appendix 4, together with the results.

After the eruption, ashes could have released to the environment up to 7 kg/m^3 of Ca. Other PTTEs could have also contribute with concentrations between 1-2 g/m^3. The modelled concentrations evidence the magnitude of the eruption, and the huge quantity of elements released.

6.7. ENVIRONMENTAL CONSIDERATIONS

The Critical Zone hold every impact caused by volcanic ash. All elements released affect surface or groundwater, and can alter ecosystems. Mobility results from column experiments suggest that episodes of biogeochemical stress can be expected after rainfall episodes. The initial impact is usually mischievous, but it may become beneficial. Showing a high capability to sequester atmospheric carbon dioxide, ash act as natural reservoir of carbon and nutrients[22].

Macronutrients like Na, Ca, K, Mg and P, and other micronutrients[23] like Fe, Ni, Cu, Zn, Mn and Cr have been mentioned several times in this work. Total contribution values confirm the high quantities of them that can be release into the environment. Those large quantities compensate the low mobility of macronutrients, giving its geochemical fluxes a fertilizing potential in continental and aquatic ecosystems, and also in oceans.

South Atlantic is one the poorest oceans in nutrient contents in the World. Due to wind direction in South America, volcanic ashes from an eruption can be transported until the Atlantic Ocean. Once there, elements are released into the oceans water, like in leaching experiments. It has been proved the exponential growth of phytoplankton after ash deposition due to raised Fe concentrations in the environment[24].

Toxicity of elements depend on its concentration, and the separation between nutrients and PTTEs is very thin. Some micronutrients unveil high mobility, that together with large contributions may become harmful for organisms. This combination results especially serious for chromium.

As and Sb present remarkable mobility and significant geochemical contributions. This makes them two PTTEs. World Health Organization fix a guideline value[25] for water consume of 20 μg/L for Sb and of 10 μg/L for As. Both of them are overcome in sample AS-04 column leachates. It is no surprise to find them in the samples, as groundwater of the northeast region of Argentina has been traditionally affected by these elements. Several studies confirm its presence, both in land and water environments[26,27]; as well as its volcanic origin. For both elements, toxicity relapse in their bioaccumulation in organisms.

7. CONCLUSIONS

Leaching tests confirm their potential to assess the geochemical hazard of volcanic ashes. Results show the release of large amounts of elements into the Critical Zone, even after thousands of years after the eruption. Total contribution values, with contributions up to $1x10^9$ Mg, also suggests the great magnitude of the Cerro Blanco eruption.

Whole-rock analysis and X-ray diffractograms conclude that all four samples come from the same volcanic episode, the Cerro Blanco eruption. Bulk composition and batch tests of sample M-508 additionally suggest external contamination. In line with archaeological hypothesis about the studied caves, anthropogenic contributions because of human occupation are proposed.

SEM images let appreciate differences in appearance between inside and outside samples, being the quantity of smallest particulate matter of ash the most significant one. Batch experiments results are not conclusive about those differences, rather than showing similar behaviour between samples.

Column experiments are key to compare samples expose to different grain sizes. Leachates concentrations and mobility coefficients between inside and outside samples confirm the differences appreciated in SEM images. The trends in which elements are grouped give a visual image of its behaviour as a result of differences in grain size and weathering processes.

Water leaching results demonstrate the huge geochemical fluxes generated when ash-water interaction take place. These are released to the environment, affecting both land and aquatic ecosystems. It is proved the rapid release of most soluble compounds, as well as major components. Although, the mobility of the elements is not exceptionally high.

Several nutrients are part of those geochemical fluxes, proving the fertilizing potential of volcanic ashes. High concentrations in solution of some micronutrients (especially of chromium), together with high mobility, may became them into PTTEs. Other harmful elements present in the studied ashes are arsenic and antimony. These two elements suppose the most sever concerns for local environment.

8. REFERENCES AND NOTES

(1) Schmincke, H.-U. *Volcanism*, 1st ed.; Springer: Berlin, 2004.

(2) Fernandez-Turiel, J. L.; Perez-Torrado, F. J.; Rodriguez-Gonzalez, A.; Saavedra, J.; Carracedo, J. C.; Rejas, M.; Lobo, A.; Osterrieth, M.; Carrizo, J. I.; Esteban, G.; et al. The Large Eruption 4.2 Ka Cal BP in Cerro Blanco, Central Volcanic Zone, Andes: Insights to the Holocene Eruptive Deposits in the Southern Puna and Adjacent Regions. *Estudios Geológicos* **2019**, *75* (1), 1–31.

(3) Wygel, C. M.; Peters, S. C.; McDermott, J. M.; Sahagian, D. L. Bubbles and Dust: Experimental Results of Dissolution Rates of Metal Salts and Glasses From Volcanic Ash Deposits in Terms of Surface Area, Chemistry, and Human Health Impacts. *GeoHealth* **2019**, 1–18.

(4) Heiken, G.; Wohletz, K. *Volcanic Ash*, 2nd ed.; University of California Press: Berkeley, 1992.

(5) Delmelle, P.; Lambert, M.; Dufrêne, Y.; Gerin, P.; Óskarsson, N. Gas/Aerosol–Ash Interaction in Volcanic Plumes: New Insights from Surface Analyses of Fine Ash Particles. *Earth Planet. Sci. Lett.* **2007**, *259* (1), 159–170.

(6) Witham, C. S.; Oppenheimer, C.; Horwell, C. J. Volcanic Ash-Leachates: A Review and Recommendations for Sampling Methods. *J. Volcanol. Geotherm. Res.* **2005**, *141* (3), 299–326.

(7) Mueller, S. B.; Ayris, P. M.; Wadsworth, F. B.; Kueppers, U.; Casas, A. S.; Delmelle, P.; Taddeucci, J.; Jacob, M.; Dingwell, D. B. Ash Aggregation Enhanced by Deposition and Redistribution of Salt on the Surface of Volcanic Ash in Eruption Plumes. *Sci. Rep.* **2017**, *7*, 45762.

(8) Ayris, P. M.; Delmelle, P. The Immediate Environmental Effects of Tephra Emission. *Bull. Volcanol.* **2012**, *74* (9), 1905–1936.

(9) *Basic Research Opportunities in Earth Science*, 1st ed.; National Research Council, Ed.; The National Academies Press: Washington, D.C., 2001.

(10) Landis, W. G.; Yu, M.-H. *Introduction to Environmental Toxicology: Impacts of Chemicals upon Ecological System*, 3rd ed.; Lewis Publishers: Boca Raton, 2004.

(11) Maher, K.; Mayer, K. U. Tracking Diverse Minerals, Hungry Organisms, and Dangerous Contaminants Using Reactive Transport Models. *Elements* **2019**, *15* (2), 81–86.

(12) Ruggieri, F.; Saavedra, J.; Fernandez-Turiel, J. L.; Gimeno, D.; Garcia-Valles, M. Environmental Geochemistry of Ancient Volcanic Ashes. *J. Hazard. Mater.* **2010**, *183* (1), 353–365.

(13) Ruggieri, F.; Fernandez-Turiel, J. L.; Saavedra, J.; Gimeno, D.; Polanco, E.; Amigo, A.; Galindo, G.; Caselli, A. Contribution of Volcanic Ashes to the Regional Geochemical Balance: The 2008 Eruption of Chaitén Volcano, Southern Chile. *Sci. Total Environ.* **2012**, *425*, 75–88.

(14) Ruggieri, F. Environmental Mobility of Potentially Toxic Trace Elements of Andean Volcanic Ashes, Doctoral Thesis, University of Barcelona, 2011.

(15) Misra, K. C. *Introduction to Geochemistry: Principles and Applications*, 1st ed.; Wiley-Blackwell: Chichester, 2012.

(16) Playà, E.; Aulinas, M. *Pràctiques de Geoquímica. Grau en Química*; Universitat de Barcelona: Barcelona, 2019.
(17) Pintar, E. Continuidades e hiatos ocupacionales durante el Holoceno Medio en el borde oriental de la Puna Salada, Antofagasta de la Sierra, Argentina. *Chungara* **2014**, *46* (1), 51–71.
(18) Cabré, J.; Aulinas, M.; Rejas, M.; Fernandez-Turiel, J. L. Volcanic Ash Leaching as a Means of Tracing the Environmental Impact of the 2011 Grímsvötn Eruption, Iceland. *Environ. Sci. Pollut. Res.* **2016**, *23* (14), 14338–14353.
(19) Oelkers, E. H.; Golubev, S. V.; Chairat, C.; Pokrovsky, O. S.; Schott, J. The Surface Chemistry of Multi-Oxide Silicates. *Geochim. Cosmochim. Acta* **2009**, *73* (16), 4617–4634.
(20) Dominy, S.; Platten, I.; Raine, M. Grade and Geological Continuity in High-Nugget Effect Gold-Quartz Reefs: Implications for Resource Estimation and Reporting. *Trans. Inst. Min. Metall., Sect. B* **2003**, *112*, 239–259.
(21) White, W. M. *Geochemistry*, 1st ed.; Johns Hopkins University Press: Baltimore, 2001.
(22) Fiantis, D.; Ginting, F.; Nelson, M.; Minasny, B. Volcanic Ash, Insecurity for the People but Securing Fertile Soil for the Future. *Sustainability* **2019**, *11*, 3072.
(23) Railsback, L. B. An Earth Scientist's Periodic Table of the Elements and Their Ions. *Geology* **2003**, *31* (9), 737–740.
(24) Browning, T. J.; Bouman, H. A.; Henderson, G. M.; Mather, T. A.; Pyle, D. M.; Schlosser, C.; Woodward, E. M. S.; Moore, C. M. Strong Responses of Southern Ocean Phytoplankton Communities to Volcanic Ash. *Geophys. Res. Lett.* **2014**, *41* (8), 2851–2857.
(25) *Guidelines for Drinking-Water Quality*, 4th ed.; World Health Organization, Ed.; WHO Library Cataloguing-in-Publication Data; World Health Organization: Geneva, 2011.
(26) Miravet, R.; López-Sánchez, J. F.; Rubio, R.; Smichowski, P.; Polla, G. Speciation Analysis of Antimony in Extracts of Size-Classified Volcanic Ash by HPLC–ICP-MS. *Anal. Bioanal. Chem.* **2007**, *387* (5), 1949–1954.
(27) McClintock, T. R.; Chen, Y.; Bundschuh, J.; Oliver, J. T.; Navoni, J.; Olmos, V.; Lepori, E. V.; Ahsan, H.; Parvez, F. Arsenic Exposure in Latin America: Biomarkers, Risk Assessments and Related Health Effects. *Sci. Total Environ.* **2012**, *429*, 76–91.

9. ACRONYMS

a.s.l.: above sea level

cal BP: calibrated years before present

CBVC: Cerro Blanco volcanic complex

CVZ: central volcanic zone

ka: kilo-year

LoD: limit of detection

LOI: loss on ignition

M: eruption mass

PP: polypropylene

PTTE: potential toxic trace elements

PVDF: polyvinylidene difluoride

RML: relative mass leached

rpm: revolutions per minute

RTM: reactive transport models

SC: specific conductivity

TC: total contribution

V_{DRE}: dens-rock equivalent volume

VEI: volcanic explosive index

ρ_{DRE}: dens-rock equivalent density

APPENDICES

APPENDIX 1: XRD AND SEM IMAGES

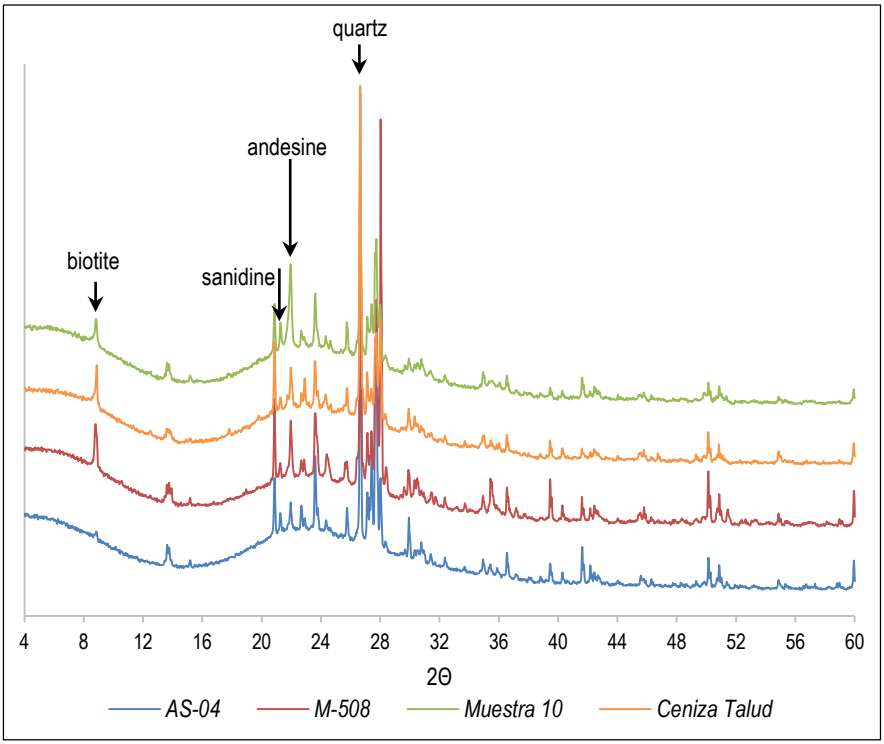

Fig. A1.1: X-Ray diffraction patterns of studied volcanic ash samples overlapped into one single diffractogram. The curvilinear shape of baseline patterns is due to the high content of glass.

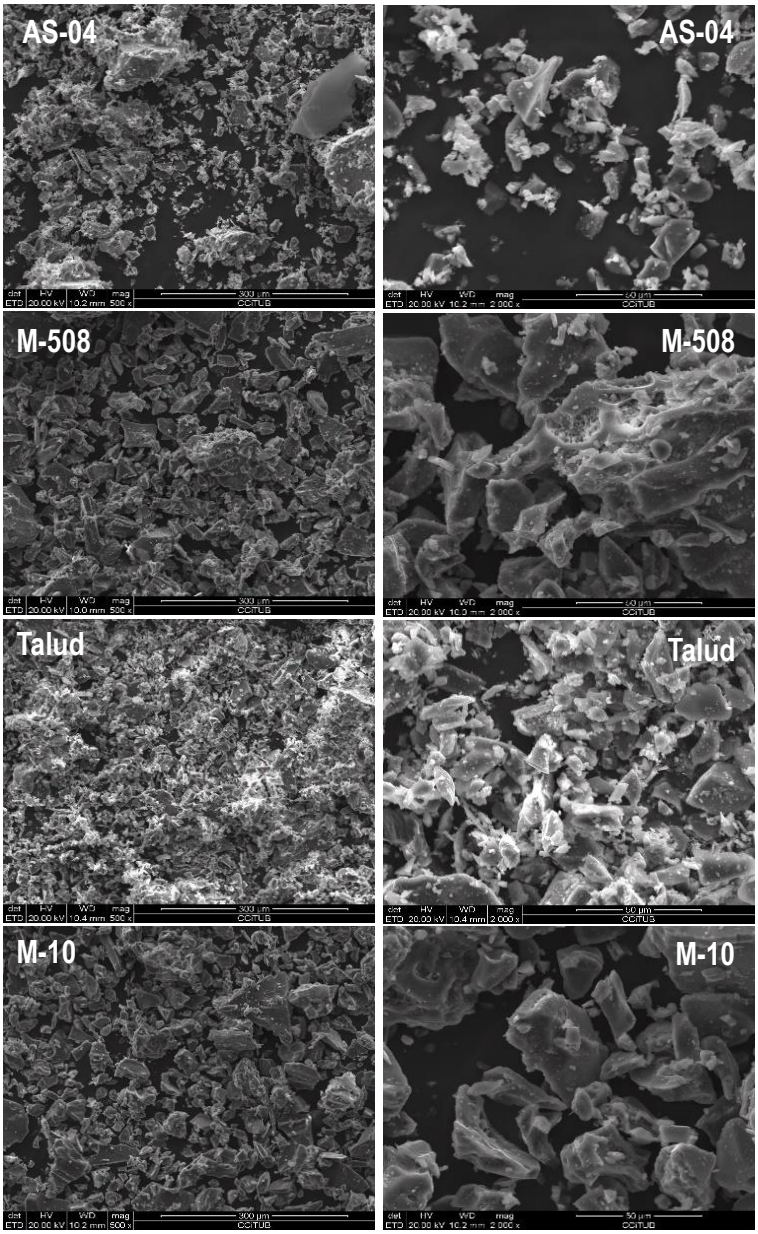

Fig. A1.2: SEM images taken with ETD detector of studied volcanic ash samples at 500 (left) and 2000 (right) magnifications ("Talud" and "M-10" as abbreviation of "Ceniza Talud" and "Muestra 10", respectively).

APPENDIX 2: BATCH TESTS RESULTS

Table A2.1: Relative mass leached (RML) and total contribution (TC) of samples "Ceniza Talud" and "Muestra 10". For RML values, green color for moderately mobile, orange for low mobile and red for extremely low mobile elements. Only represented elements whose concentrations are above LoD; symbol "/" designate non-detected elements on water leachates.

	Ceniza Talud		Muestra 10	
Element	**RML**	**TC** [Mg x10^4]	**RML**	**TC** [Mg x10^4]
Ca	0.0836%	14420	0.0514%	8866
Mg	0.0133%	2297	0.0278%	4799
Na	0.0204%	3526	0.0030%	514
K	0.0068%	1169	0.0089%	1533
Si	0.0013%	219	0.0005%	93
Ti	0.0014%	234	/	/
Al	0.0001%	15	0.0001%	18
Fe	0.0108%	1858	0.0137%	2355
Mn	0.0006%	96	/	/
P	0.0608%	10495	0.0304%	5247
Li	0.0263%	4.54	0.0009%	0.16
Be	0.0053%	0.91	0.0048%	0.84
Sc	0.0071%	1.23	/	/
Cr	0.1551%	26.75	0.1914%	33.02
Ni	0.2046%	35.30	0.2111%	36.42
Cu	0.0641%	11.06	0.0681%	11.74
Zn	0.0655%	11.30	0.0860%	14.83
Ge	0.0106%	1.83	/	/
As	0.0407%	7.02	0.0057%	0.99
Rb	0.0001%	0.02	0.0014%	0.24
Sr	0.0626%	10.80	0.0621%	10.71
Zr	0.0012%	0.20	0.0012%	0.20
Sn	0.6397%	110.35	0.6522%	112.51
Sb	0.0363%	6.27	0.0452%	7.81
Ba	0.0064%	1.10	0.0071%	1.22
La	/	/	0.0014%	0.24
Ce	0.0006%	0.10	0.0011%	0.18
Nd	0.0011%	0.19	/	/
Hf	0.0059%	1.03	0.0061%	1.05
Pb	0.0039%	0.68	0.0052%	0.90

Table A2.2: RML and TC of samples AS-04 and M-508. For RML values, green color for moderately mobile, orange for low mobile and red for extremely low mobile elements. Only represented elements whose concentrations are above LoD; symbol "/" designate non-detected elements on water leachates.

	AS-04		M-508	
Element	**RML**	**TC** [Mg x10^4]	**RML**	**TC** [Mg x10^4]
Ca	0.1538%	26535	0.2567%	44288
Mg	/	/	0.2840%	48989
Na	0.0061%	1058	0.4275%	73744
K	0.0070%	1211	0.0217%	3747
Si	0.0003%	46	0.0002%	27
Ti	0.0014%	241	0.0004%	62
Al	0.0003%	50	0.0001%	13
Fe	0.0164%	2835	0.0075%	1300
Mn	0.0006%	104	0.0167%	2884
P	0.0949%	16377	0.0328%	5655
Li	0.0042%	0.73	0.0420%	7.25
Be	/	/	0.0063%	1.09
Sc	0.0198%	3.42	/	/
Cr	0.1321%	22.78	0.0537%	9.27
Co	/	/	0.0318%	5.49
Ni	0.8000%	138.00	0.0945%	16.30
Cu	0.1414%	24.39	0.2564%	44.22
Zn	0.0979%	16.88	0.0604%	10.43
As	0.0522%	9.00	0.1320%	22.76
Rb	0.0009%	0.15	0.0096%	1.65
Sr	0.1103%	19.02	0.1237%	21.34
Y	/	/	0.0030%	0.53
Zr	0.0017%	0.30	0.0030%	0.52
Sn	0.7083%	122.17	0.7785%	134.29
Sb	0.0414%	7.13	0.0446%	7.69
Ba	0.0160%	2.75	0.0091%	1.56
La	0.0713%	12.30	0.0021%	0.37
Ce	0.0238%	4.11	0.0017%	0.30
Nd	/	/	0.0028%	0.48
Gd	0.0058%	1.00	/	/
Hf	0.0067%	1.15	0.0107%	1.85
Pb	0.0058%	1.01	0.0067%	1.16
Th	/	/	0.0011%	0.19
U	/	/	0.0016%	0.27

APPENDIX 3: COLUMN TESTS RESULTS

Table A3.1: RML and TC of samples AS-04 and "Muestra 10". For RML values, blue color for mobile, green for moderately mobile, orange for low mobile and red for extremely low mobile elements. Only represented elements whose concentrations are above LoD; symbol "/" designate non-detected elements on water leachates.

	AS-04		Muestra 10	
Element	**RML**	**TC** [Mg x10⁴]	**RML**	**TC** [Mg x10⁴]
Ca	0,9965%	171904	0,1052%	18151
Mg	/	/	0,0698%	12032
Na	0,0201%	3473	0,0063%	1092
K	0,0126%	2182	0,0141%	2432
Si	0,0027%	464	0,0020%	342
Ti	0,0013%	222	0,0010%	167
Al	0,0038%	664	0,0013%	219
Fe	0,0140%	2407	0,0102%	1754
Mn	0,0031%	529	0,0027%	469
P	0,9895%	170681	0,2912%	50238
Li	0,0142%	2,44	0,0023%	0,39
Be	0,0024%	0,41	0,0019%	0,33
Sc	0,0006%	0,10	0,0007%	0,12
V	0,0201%	3,47	0,0111%	1,91
Cr	0,1408%	24,28	0,1214%	20,94
Co	0,0191%	3,29	0,0084%	1,44
Ni	0,9550%	164,74	0,1932%	33,32
Cu	0,3026%	52,20	0,0778%	13,43
Zn	0,0974%	16,80	0,0479%	8,27
Ga	0,0008%	0,13	0,0009%	0,15
Ge	0,0036%	0,62	0,0015%	0,26
As	0,2239%	38,62	0,0119%	2,06
Rb	0,0028%	0,48	0,0043%	0,74
Sr	0,5169%	89,16	0,1355%	23,38
Y	0,0008%	0,14	0,0030%	0,52
Zr	0,0014%	0,24	0,0013%	0,22
Sn	0,0746%	12,86	0,0317%	5,47
Sb	1,3267%	228,85	0,0169%	2,91
Cs	0,0004%	0,08	0,0009%	0,16
Ba	0,0233%	4,02	0,0161%	2,78

Table A3.1: (continued)

Element	AS-04		Muestra 10	
	RML	TC [Mg x10^4]	RML	TC [Mg x10^4]
La	0,0009%	0,16	0,0050%	0,86
Ce	0,0013%	0,23	0,0051%	0,87
Pr	0,0005%	0,09	0,0043%	0,73
Nd	0,0010%	0,17	0,0060%	1,04
Sm	0,0004%	0,07	0,0044%	0,77
Gd	0,0005%	0,09	0,0045%	0,78
Tb	0,0003%	0,06	0,0050%	0,86
Dy	0,0003%	0,05	0,0040%	0,69
Ho	0,0003%	0,05	0,0041%	0,71
Er	0,0001%	0,03	0,0009%	0,16
Tm	/	/	0,0002%	0,03
Yb	0,0001%	0,02	0,0004%	0,07
Hf	0,0054%	0,93	0,0045%	0,78
Pb	0,0047%	0,81	0,0045%	0,77
Th	0,0003%	0,05	0,0008%	0,14
U	0,0031%	0,53	0,0009%	0,15

APPENDIX 4: THEORETICAL MODEL OF PRECIPITATION

As the eruption took place around 4,200 years ago, a theoretical model was developed to simulate the effects of rain episodes on ashes. With column data results (volume of percolated water and ash cartridge surface), an equivalent precipitation measure was calculated for flow-through experiments.

Annual precipitation for Antofagasta de la Sierra valley is 65mm (Table A4.1) (extracted from web https://en.climate-data.org). It was divided per the equivalent precipitation to obtain the equivalent years of flow-through experiment.

Elemental leachate compositions were multiplied by ρ_{DRE} and then divided per the equivalent years to obtain a concentration value expressed as $mg/m^3 \cdot year$. Those results are shown in Table A4.2 as "flow-through experiment". If an average annual precipitation of 65mm is considered for 4,200 years, and then applying a conversion factor from milligrams to grams, the results for theoretical model are obtained.

These results refer to the theoretical minimal quantities that could be released to environment after thousands of years of exposition to climate conditions. Obtained values were calculated from column leachate compositions for sample AS-04 (Puna region).

Table A4.1: Theoretical model of precipitation for Puna region. Precipitation values expressed as mm (L/m^2).

	Puna region
Annual precipitation (Antofagasta de la Sierra) [mm]	65
Flow-through experiment (equivalent precipitation) [mm]	3053
Equivalent years of flow-through experiment [years]	47

Table A4.2: Element concentrations for major components and some micro-nutrients and PTTEs for theoretical model of precipitation.

	Puna region	
Element	**Flow-through experiment** [mg/m^3·year]	**Theoretical model** [g/m^3]
Ca	2301,7	9666,9
Mg	18,2	76,4
Na	213,6	897,2
K	191,4	803,9
Si	479,3	2012,9
Ti	0,4	1,5
Al	111,7	469,1
Fe	24,6	103,3
Mn	0,7	2,9
P	21,5	90,2
Cr	0,3	1,1
Ni	0,5	2,0
Cu	0,3	1,2
Zn	1,7	7,3
As	0,5	2,2
Sr	5,8	24,2
Sb	0,3	1,2